Computer Simulation and Characterization of Solar Energy and Photovoltaic Cells

Amira A.A.Diab[1], S.M.El-Ghanam[2], S.A.Kamh[2] and F.A.S.Soliman[3]
1- M.Sc. Student, Physics Dept., Faculty of Women for Arts, Science, and Education, Ain-Shams Univ., Cairo, Egypt.
2- Physics Dept., Faculty of Women for Arts, Science and Education, Ain-Shams Univ., Cairo, Egypt.
3- Nuclear Materials Authority, P. O. Box 530-Maadi-11728, Cairo, Egypt.

Abstract— Detailed computer simulation based study of photovoltaic cells/ modules using circuit simulator PVEducation S/W package was presented in this paper and used to simulate a circuit based model or PV cells/ modules and then to conduct behavioral study under varying conditions of solar insolation including temperature, diode model parameters, series and shunt resistance, solar energy ……etc. The study is very helpful in clearly outlining the principles and the intricacies of PV cells/modules and may surely be used to verify impact of different topologies and control techniques on the performance of different types of PV system. To put the simulation study on firm footing, a comparative study was carried out with a previous work done by the authors, where an excellent agreement was obtained.

Index Terms— Computer Simulation, diode model parameters, photovoltaic cells, PVEducation, solar insolation and temperature.

1 Introduction to Simulation

The equations that describe solar cell can be solved analytically or numerically [1-3]. While the analytical equations are easier to solve by hand and give great insight into cell operation, but they become difficult to solve as more factors of cell operation are included. In the past, it was common to rewrite the equations slightly to simplify the solution to solve specific cases; however, such methods are time consuming. In this concern, computer speeds have increased (and memory for 2D cases), so it is now easier to write a general solver that applies to most cases. There are an enormous number of packages for modeling semi-conductor devices. However most of these packages either don't consider light generation or only partially include light generation effects. Even for packages specifically designed for simulating solar cells there exist a wide range of solvers both in house and commercially available for simulating solar cell operation. Most of these packages have fairly similar basic module and it comes down to how fast they are, how easy they are to use and how many effects they model.

The basic operation of a modeling program consists of setting up the model with user defined parameters, a generation of nodes to solve, then iterating to produce a solution that is consistent with all the nodes [4-6]. Finally, the two device modeling programs commonly within the photovoltaic community: PC1D for one-dimensional modeling and DESSIS for two dimensional modeling.

1.1 PVEducation Software Package

PVEducation S/W package (PC1D) is the most commonly used S/W of the commercially available solar cell modeling programs [7, 8]. Its success is based on its speed, user interface and continual updates to the latest cell models. It is used to simulate new device performance and also for new users to develop an understanding of device physics. PC1D is now available free of charge from the University of NSW. The raw source code of PC1D is now available on Source-Forge for programmers and developers. PV Light house has more PC1D resources including a batch file generator. solar cell modeling programs [7, 8]. Its success is based on its speed, user interface and continual updates to the latest cell

2 Effects of Illumination Intensity

2.1 Low Light Intensity

Solar cells experience daily variations in light intensity, with the incident power from the sun varying between 0 and 1.0 kW/m2. At low light levels, the effect of the shunt resistance becomes increasingly important [9-13]. As the light intensity decreases, the bias point and current through the solar cell also decreases and the equivalent resistance of the solar cell may begin to approach the shunt resistance. When these two resistances are similar, the fraction of the total current flowing through the shunt resistance increases, thereby increasing the fractional power loss due to shunt resistance. Consequently, under cloudy conditions, a solar cell with a high shunt resistance retains a greater fraction of its original power than a solar cell with a low shunt resistance. Finally, Fig. (1) shows the output characteristics of solar panel, plotted under different illumination levels up 2 suns, at R_s = 1.0 Ω, R_{sh} = 10 kΩ and the simulation plots of short circuit current density-and open circuit voltage-dependences on low illumination levels, for ideal -and real -solar cells (R_s=1.0 Ω, R_{sh} = 10 kΩ).

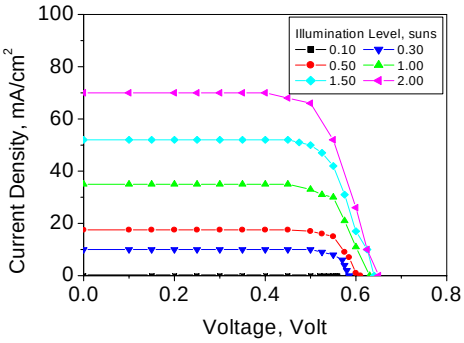

(a)

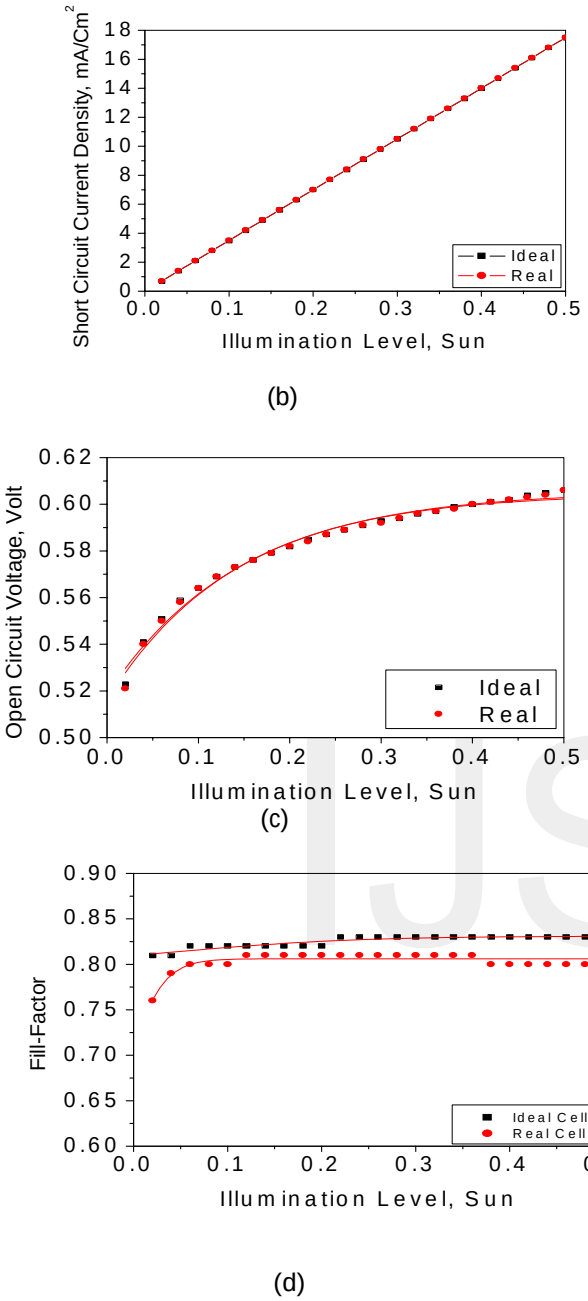

Fig.1. Simulation plots of the effects of illumination level on the output characteristics (a), short circuit current density (b), open circuit voltage (c) and fill-factor (d) for ideal-and real-solar cells, plotted at R_s=1.0 Ω, R_{sh}=10 kΩ.

2.2 CONCENTRATORS

A concentrator is a solar cell designed to operate under illumination greater than 1.0 sun. The incident sunlight is focused or guided by optical elements such that a high intensity light beam shines on a small solar cell [14]. Concentrators have several potential advantages, including a higher efficiency potential than a one-sun solar cell and the possibility of lower cost. The short-circuit current from a solar cell depends linearly on light intensity, such that a device operating under 10 suns would have 10 times the short-circuit current as the same device under one sun operation. However, this effect does not provide an efficiency increase, since the incident power also increases linearly with concentration. Instead, the efficiency benefits arise from the logarithmic dependence of the open-circuit voltage on short circuit [5]. Therefore, under concentration, Voc increases logarithmically with light intensity, as shown in Eq. (1). Finally, Fig. (2) show the effects of high illumination levels on short circuit current density, open circuit voltage, and fill-factor for ideal -and real - solar cells (R_s=1.0 Ω, R_{sh}=10 kΩ).

$$V_{oc}' = \frac{nkT}{q}\ln\left(\frac{XI_{sc}}{I_0}\right) = \frac{nkT}{q}\left[\ln\left(\frac{I_{sc}}{I_0}\right) + \ln X\right] = V_{oc} + \frac{nkT}{q}\ln X \quad (1)$$

Where, X is the concentration of sunlight.

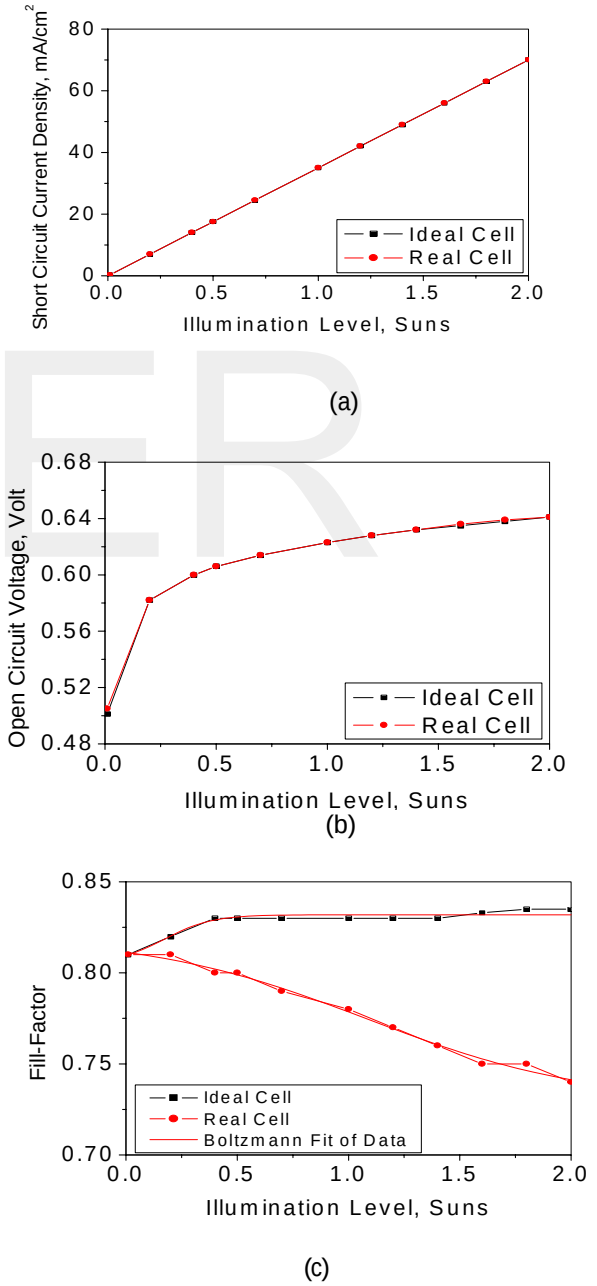

Fig. (2): Effects of high illumination levels on short circuit current density (a), open circuit voltage (b) and fill- factor (c) for ideal-and real-solar cells (R_s=1.0 Ω, R_{sh}=10 kΩ).

2.3 QUANTUM EFFICIENCY

The "quantum efficiency" (Q.E.) is the ratio of the number of carriers collected by the solar cell to the number of photons of a given energy incident on the solar cell [15]. If all photons of a certain wavelength are absorbed and the resulting minority carriers are collected, then the quantum efficiency at that particular wavelength is unity. The quantum efficiency for photons with energy below the band gap is zero. A quantum efficiency curve for an ideal solar cell is shown in Fig. (3).

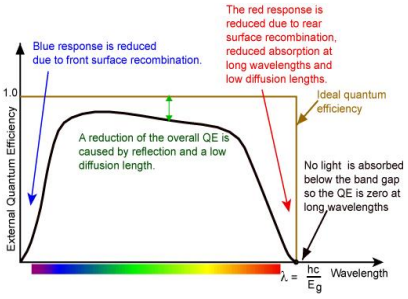

Fig. (3): Quantum efficiency of a silicon solar cell.

While quantum efficiency ideally has the square shape, the quantum efficiency for most solar cells is reduced due to recombination effects. For example, front surface passivation affects carriers generated near the surface, and since blue light is absorbed very close to the surface, high front surface recombination will affect the "blue" portion of the quantum efficiency. Similarly, green light is absorbed in the bulk of a solar cell and a low diffusion length will affect the collection probability from the solar cell bulk and reduce the quantum efficiency in the green portion of the spectrum. The quantum efficiency can be viewed as the collection probability due the generation profile of a single wavelength, integrated over the device thickness and normalized to the incident number of photons.

The "external" quantum efficiency of a silicon solar cell includes the effect of optical losses such as transmission and reflection. However, it is often useful to look at the quantum efficiency of the light left after the reflected and transmitted light has been lost. "Internal" quantum efficiency refers to the efficiency with which photons that are not reflected or transmitted out of the cell can generate collectable carriers. By measuring the reflection and transmission of a device, the external quantum efficiency curve can be corrected to obtain the internal quantum efficiency curve. Finally, Fig. (4) shows the quantum efficiency of silicon solar panel, plotted at different emitter diffusion length, L_P. (a), base diffusion length, L_n (b), front surface recombination velocity, FSRV (c) and rear surface recombination velocity, RSRV (d).

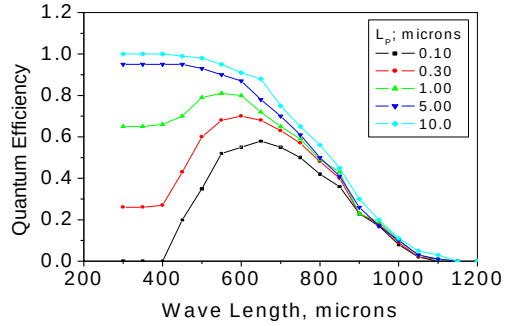

(a)

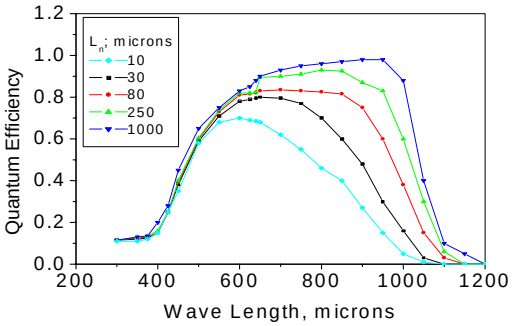

(b)

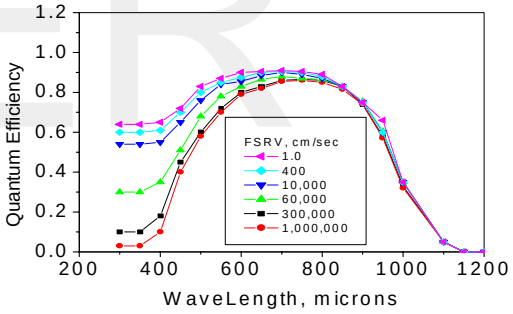

(c)

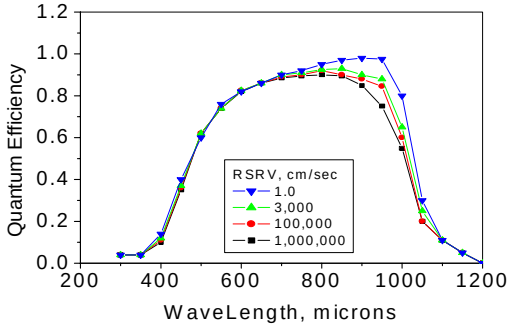

(d)

Fig. 4. Quantum efficiency of silicon solar panel, plotted at different emitter diffusion length (a) base diffusion length (b), front surface recombination velocity, FSRV(c) and, rear surface recombination velocity RSRV (d).

3 Resistive Effects of Solar Cells

3.1 Characteristic Resistance

The characteristic resistance of a solar cell is the output resistance of the solar cell at its maximum power point (Fig. 5). If the resistance of the load is equal to the characteristic resistance of the solar cell, then the maximum power is transferred to the load and the solar cell operates at its maximum power point. It is a useful parameter in solar cell analysis, particularly when examining the impact of parasitic loss mechanisms [16].

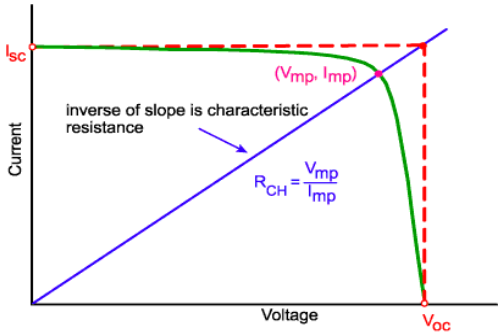

Fig. 5. Characteristic resistance of a solar cell.

The characteristic resistance of a solar cell is the inverse of the slope of the line, shown in the Fig. (5), which can be given as (Eq. 2):

$$R_{CH} = \frac{V_{MP}}{I_{MP}} \text{..... .....(2)}$$

It can alternately be given as an approximation where:

$$R_{CH} = \frac{V_{OC}}{I_{SC}} \text{.....(3)}$$

3.1.1 Parasitic Resistance

Resistive effects in solar cells reduce the efficiency of the solar cell by dissipating power in the resistances. The most common parasitic resistances are series resistance and shunt resistance. The inclusion of the series and shunt resistance on the solar cell model is shown in Fig. (6).

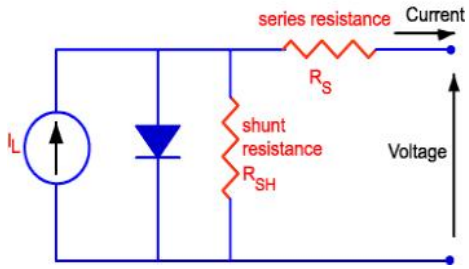

Fig. 6. Parasitic series and shunt resistances in a solar cell circuit.

In most cases and for typical values of shunt and series resistance, the key impact of parasitic resistance is to reduce the fill factor. Both the magnitude and impact of series and shunt resistance depend on the geometry of the solar cell, at the operating point of the solar cell. Since the value of resistance will depend on the area of the solar cell, when comparing the series resistance of solar cells which may have different areas, a common unit for resistance is in Ω.cm². This area-normalized resistance results from replacing current with current density in Ohm's law as shown below (Eq. 4):

$$R'(\Omega cm^2) = \frac{V}{J} \text{.....(4)}$$

3.1.1.1 Series Resistance

Series resistance in a solar cell has three causes (Fig. 7): firstly, the movement of current through the emitter and base of the solar cell; secondly, the contact resistance between the metal contact and the silicon; and finally the resistance of the top and rear metal contacts. The main impact of series resistance is to reduce the fill factor, although excessively high values may also reduce the short-circuit current, where (Equ. 5):

$$I = I_L - I_0 \exp\left[\frac{q(V+IR_S)}{nkT}\right] \text{.....(5)}$$

Where,
I : cell output current,
I_L : light generated current,
V : voltage across the cell terminals,
T : temperature,
q and k are constants,
n : ideality factor, and
R_S : cell series resistance.

The formula is an example of an implicit function due to the appearance of the current, I, on both sides of the equation and requires numerical methods to solve. Finally, Fig's. (8) shows the simulated data of the effects of series resistance on the output characteristic curves (a) and output power (b) of real solar cell (R_{sh} = 10 kΩ).
It is clearly shown that series resistance does not affect the solar cell at open-circuit voltage since the overall current flow through the solar cell, and therefore through the series resistance is zero. However, near the open-circuit voltage, the (I-V) curve is strongly affected by the series resistance. A straight-forward method of estimating the series resistance from a solar cell is to find the slope of the (I-V) curve at the open-circuit voltage point.

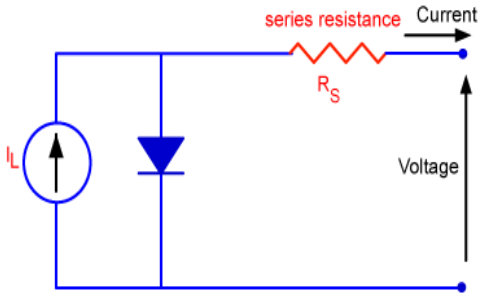

Fig. 7. Schematic of a solar cell with series resistance.

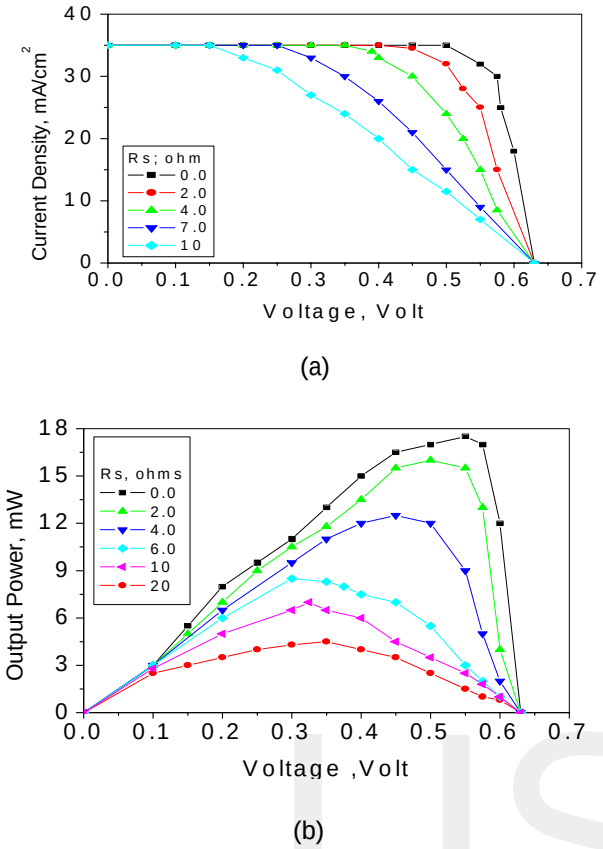

Fig. 8. Effects of series resistance on the output characteristic curves (a) and output power (b) of real solar cell (Rsh = 10 kΩ).

3.1.1.2 Shunt Resistance

Significant power losses caused by the presence of a shunt resistance, R_{SH}, are typically due to manufacturing defects, rather than poor solar cell design [17]. Low shunt resistance causes power losses in solar cells by providing an alternate current path for the light-generated current. Such a diversion reduces the amount of current flowing through the solar cell junction and reduces the voltage from the solar cell. The effect of a shunt resistance is particularly severe at low light levels, since there will be less light-generated current. The loss of this current to the shunt therefore has a larger impact. In addition, at lower voltages where the effective resistance of the solar cell is high, the impact of a resistance in parallel is large. Finally, Fig. (9) shows the circuit diagram of a solar cell including the shunt resistance (Fig. 9a) and its effects of on real solar cell characteristics, plotted at Rs=1.0 Ω (Fig. 9b). Finally, the equation for a solar cell in presence of a shunt resistance is:

$$I = I_L - I_0 \exp[qV / nkT] - VR_{SH} \quad \text{.....(6)}$$

where:
I : cell output current,
I_L : light generated current,
V : voltage across the cell terminals,
T : temperature,
q and k are constants,
n is the ideality factor, and
R_{SH} is the cell shunt resistance.

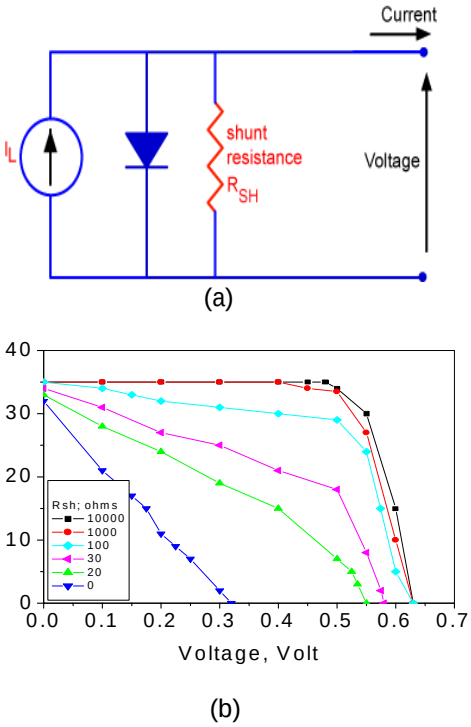

Fig. 9. Circuit diagram of a solar cell including the shunt resistance (a), and its effects of on real solar cell characteristics (b) (Rs= 1.0 Ω).

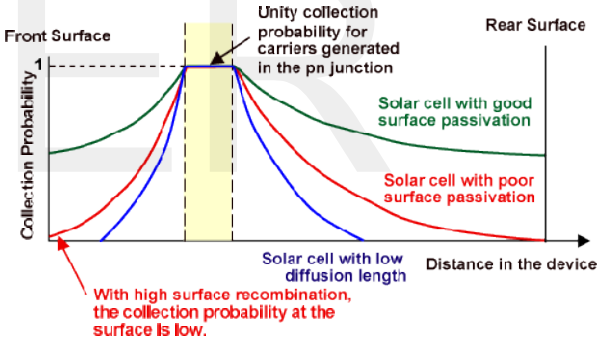

Fig. 10. Impact of surface passivation and diffusion length on collection probability

4 Collection Probability

The "collection probability" describes the probability that a carrier generated by light absorption in a certain region of the device will be collected by the p-n junction and therefore contribute to the light-generated current, but probability depends on the distance that a light-generated carrier must travel compared to the diffusion length. Collection probability also depends on the surface properties of the device. The collection probability of carriers generated in the depletion region is unity as the electron-hole pair is quickly swept apart by the electric field and are collected. Away from the junction, the collection probability drops. If the carrier is generated more than a diffusion length away from the junction, then the collection probability of this carrier is quite low. Similarly, if the carrier is generated closer to a region such as a surface with higher recombination than the junction, then the carrier will recombine. The impact of surface passivation and diffusion length on collection probability is shown in Fig. (10). Finally, Fig. (11) shows the collection probability of the base

and emitter of silicon solar panel, plotted at different front surface recombination velocity, FSRV (Fig. 11a), rear surface recombination velocity, RSRV (Fig. 11b), base diffusion length, L_n (Fig. 11c) and emitter diffusion length, L_P (Fig. 11d).

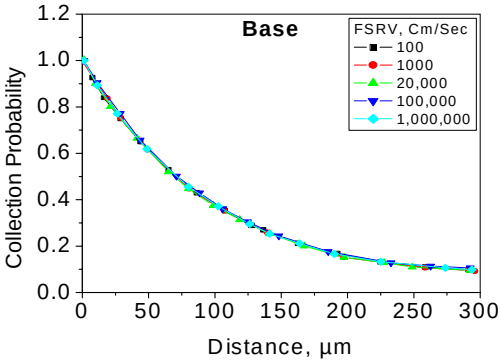

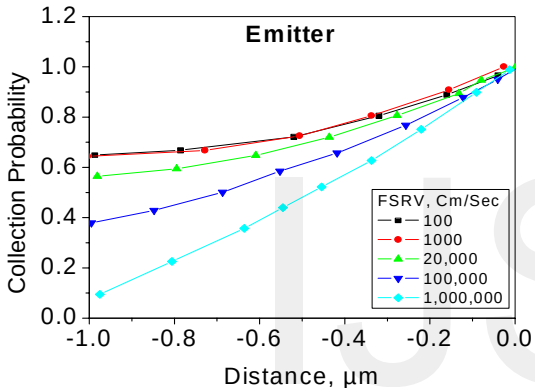

Fig.(11a)

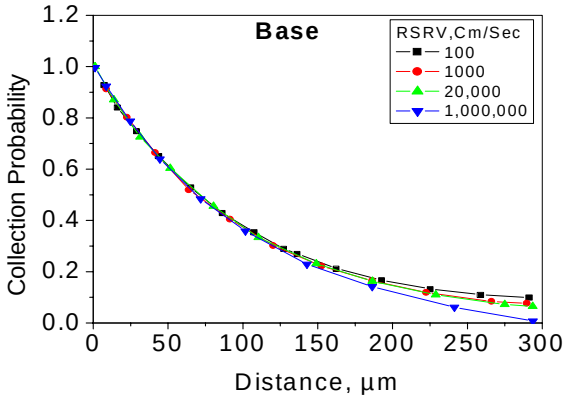

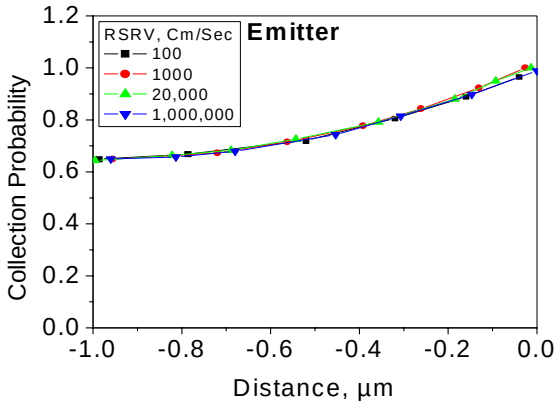

Fig. (11b)

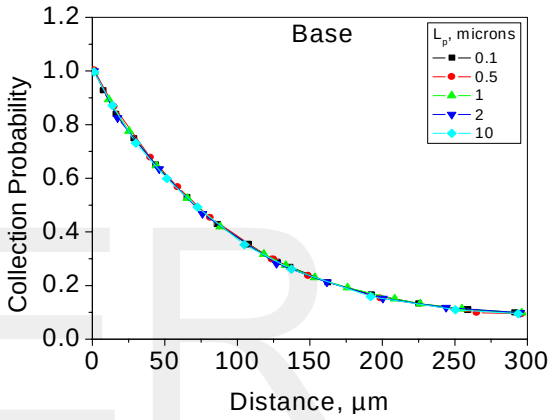

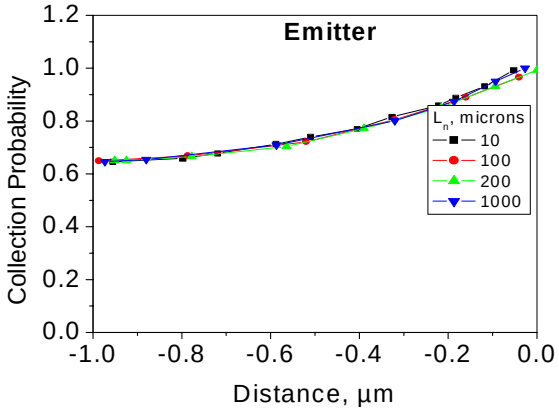

Fig.(11c)

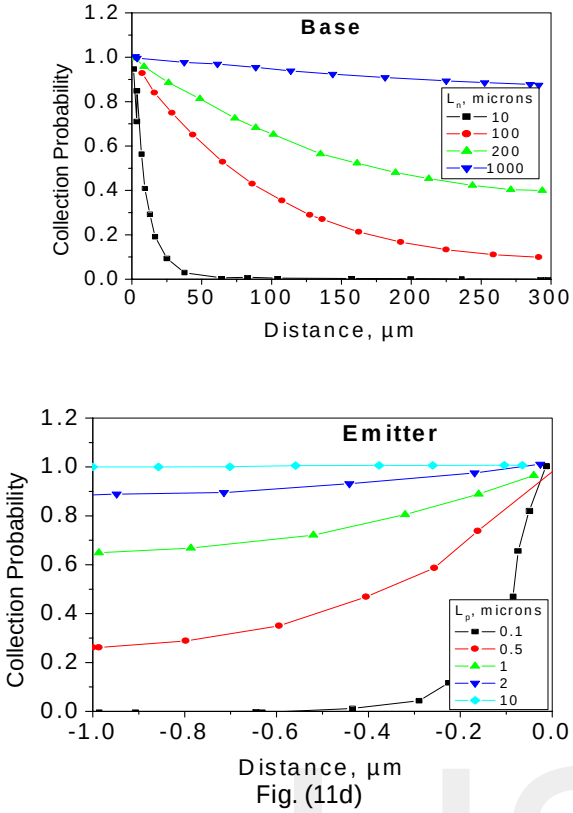

Fig. (11d)

Fig. (11): Collection probability of the base and emitter of silicon solar cell, plotted at different front surface recombination velocity, FSRV(a), base diffusion length, lRSRV (b), base diffusion length, Ln (c) and emitter diffusion length, LP (d).

The collection probability in conjunction with the generation rate in the solar cell determines the light-generated current from the solar cell. The light-generated current is the integration over the entire device thickness of the generation rate at a particular point in the device, multiplied by the collection probability at that point (Fig. 12). Eq. (7) gives the light-generated current density (J_L), with an arbitrary generation rate (G(x)) and collection probability (CP(x)), as is the generation rate in silicon due to the AM1.5 solar spectrum (Fig. 12). From which, it is clear that the carrier generation is the highest at surface of the solar cell, thus making photovoltaic devices very sensitive to surface properties.

$$I_{L=}q\int_0^W G(x)CP(x)dx = q\int_0^W[\int \alpha(\lambda)H_0\exp(-\alpha(\lambda)x)\,d\lambda]CP(x)dx \quad \ldots.(7)$$

Where,
q : electronic charge;
W : thickness of the device;
$\alpha(\lambda)$: absorption coefficient;
H_0 : number of photons at each wavelength.

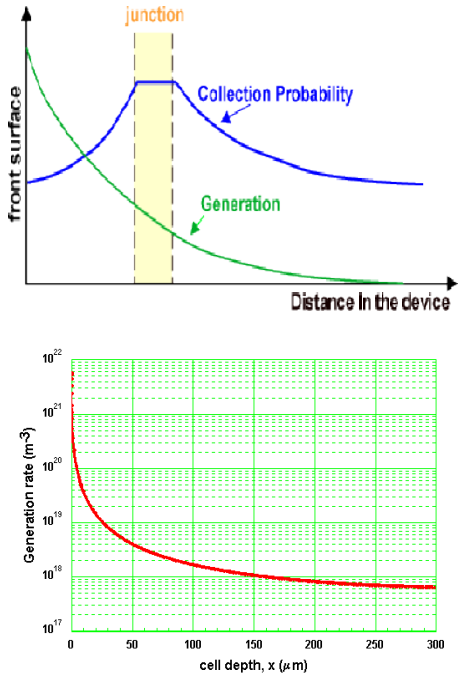

Fig. 12. Dependence of light-generated current on the generation of carriers and their collection probability (a), and the generation profile in silicon due to the AM1.5 spectrum (b).

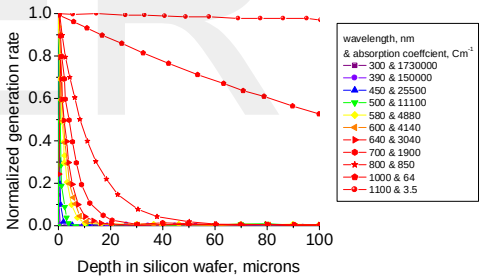

Fig. 13. Normalized generation rate at different wavelengths of light in silicon.

A non-uniform collection probability will cause a spectral dependence in the light-generated current. For example, at the surfaces, the collection probability is lower than in the bulk. Comparing the generation rates for blue, green and infrared light below, blue light is nearly completely absorbed in the first few tenths of a micron in silicon. Therefore, if the collection probability at the front surface is low, any blue light in the solar spectrum does not contribute to the light-generated current. In this concern, Fig. (13) shows the normalized generation rate at different wavelengths of light in silicon. From which, it is clear that blue light of 0.45 μm has a high absorption coefficient of 105 cm-1 and is therefore absorbed very close to the front surface. Red light at 0.8 μm and an absorption coefficient of 103 cm-1 is absorbed deeper into the cell. Infrared light at 1.10 μm with an absorption

IJSER © 2016
http://www.ijser.org

coefficient of 103 cm-1 is barely absorbed since it is close to the band gap of silicon.

5 Temperature Effects on Solar Cells

Like all other semiconductor devices, solar cells are sensitive to temperature. Increases in temp-erature reduce the band gap of a semi-conductor, thereby effecting most of the semiconductor material parameters [18]. The decrease in the band gap of a semiconductor with increasing temperature can be viewed as increasing the energy of the electrons in the material. Lower energy is therefore needed to break the bond. In the bond model of a semiconductor band gap, reduction in the bond energy also reduces the band gap. Therefore increa-sing the temperature reduces the band gap.

5.1 Temperature Effects on Intrinsic Carrier Concentration.

In a solar cell, the parameter most affected by an increase in temperature is the open-circuit voltage. The open-circuit voltage decreases with temperature because of the temperature dependence of I0. The equation for I_0 from one side of a p-n junction is given by;

$$I_0 = q.\ A.\ (D.n_i^2\ /\ L.N_D) \ldots\ldots\ldots\ldots\ldots\ldots\ldots\ldots\ldots\ldots (8)$$

Where,
q : electronic charge given in the constants page;
D : diffusivity of the minority carrier,
L : diffusion length of the minority carrier;
N_D : doping; and
n_i : intrinsic carrier concentration given for silicon.

In the above equation, many of the parameters have some temperature dependence, but the most significant effect is due to the intrinsic carrier concentration, n_i. The intrinsic carrier concentration depends on the band gap energy (with lower band gaps giving a higher intrinsic carrier concentration), and on the energy which the carriers have (with higher temperatures giving higher intrinsic carrier concentrations). Fig. (14) shows the simulated results of temperature dependence of intrinsic carrier concentration of solar cells. From which, it is clearly shown that the temperature dependence of the intrinsic carriers concentration follows a polynomial fit.

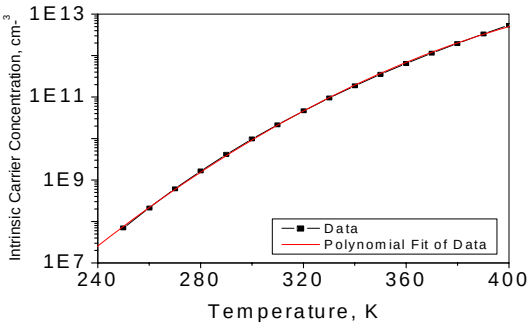

Fig. 14. Temperature effects on intrinsic concentration of silicon solar cells.

5.2 Temperature Effects on Open Circuit Voltage and Fill-Factor

The study was extended to include the simu-lation of the temperature effects on the open circuit voltage and fill-factor, applying the proposed software package (Fig. 15). The dependences of both the open circuit voltage and fill-factor on temperature were shown to follow linear decreasing functions.

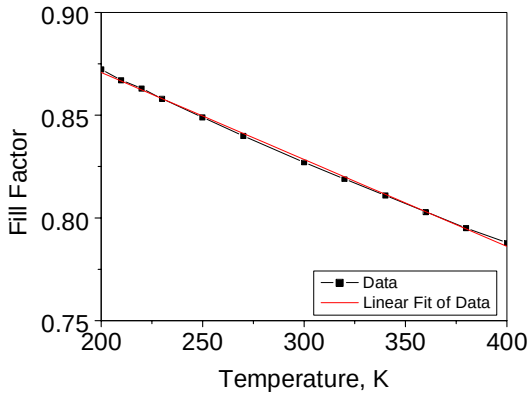

(a)

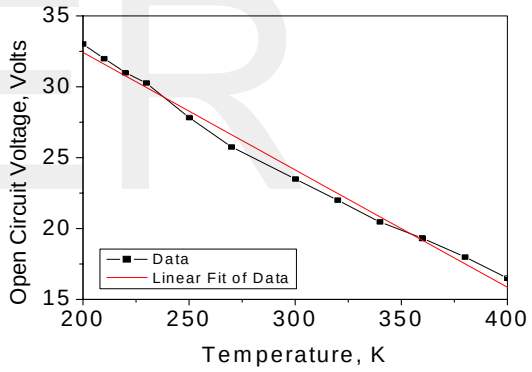

(b)

Fig. 15. Temperature effects on (a) fill factor and (b) open circuit voltage of silicon solar panel.

6 Calculations of Sun Hours.

The number of hours the sun is shining each day, that is the number of hours between sunrise and sunset each day. In latitudes above 67° the sun shines for 24 hours during part of the year (Fig. 16). Surprisingly, when averaged over the year, the sun shines an average of 12 hours per day everywhere in the world. In the northern latitudes the average intensity is lower than at the southern latitudes. In Cairo (30.0500°N, 31.2333°E), it is clearly shown that sun is shining, in average, between 10 to 14 hours (Fig. 17) [19].

IJSER © 2016
http://www.ijser.org

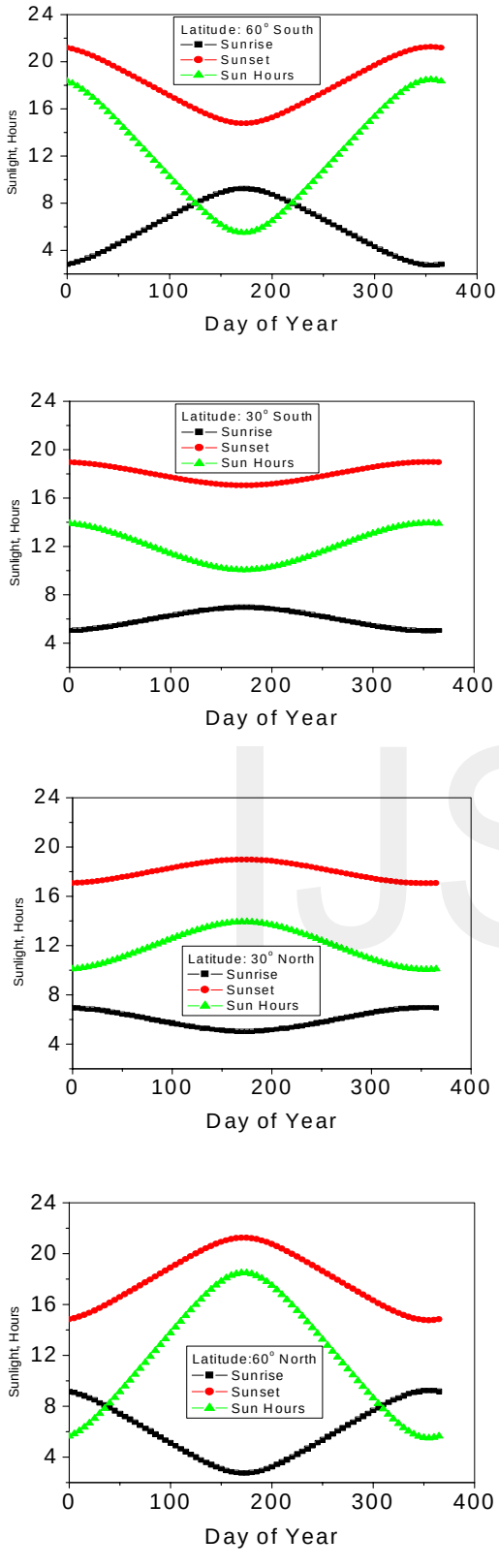

Fig. (16): Sunlight hours vs. day of year, plotted at different latitude angles

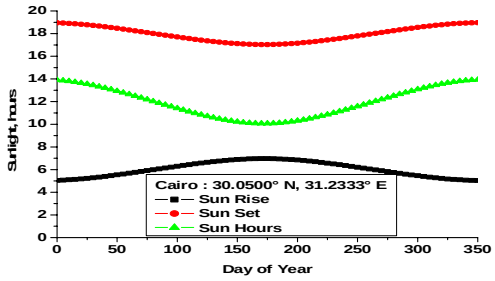

Fig. 17. Sunlight hours vs. days of year at Cairo, Egypt.

7 Direct Solar Radiation Calculations

The three curves are the incident solar insolation, the horizontal solar insolation and the solar insolation on a titled surface. The daily insolation is numerically equal to the number of sun hours in a day. The module is assumed to face the equator so that it faces South in the northern hemisphere in North in the southern hemisphere. Finally, Fig. (18) shows the solar direct radiation vs. 24 hour day time, plotted at different year months.

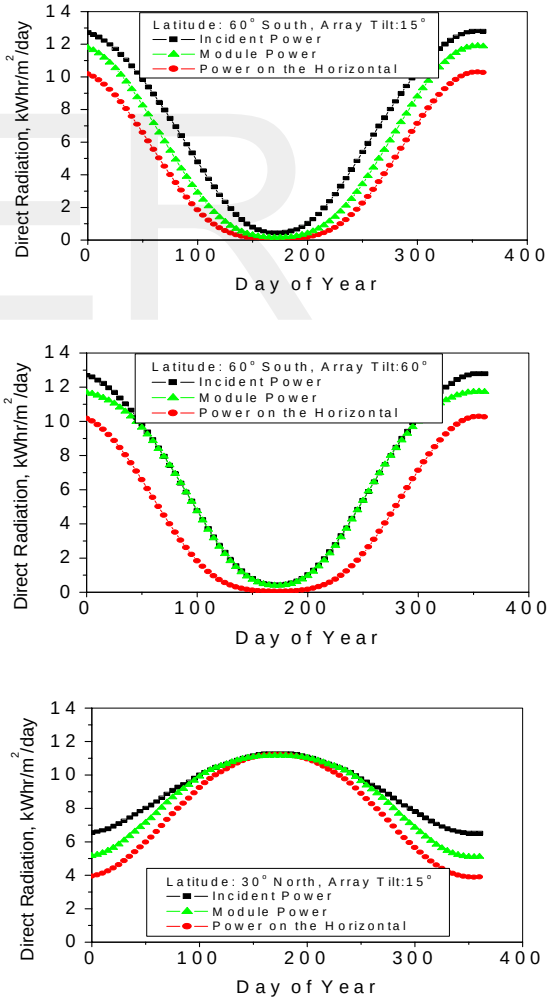

Fig. (18): Direct solar radiation vs. day of year, plotted at different latitude- and arrays angles.

IJSER © 2016
http://www.ijser.org

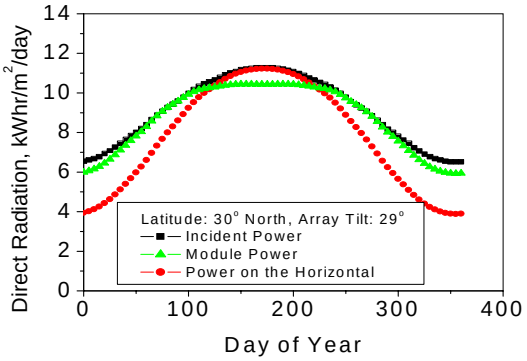

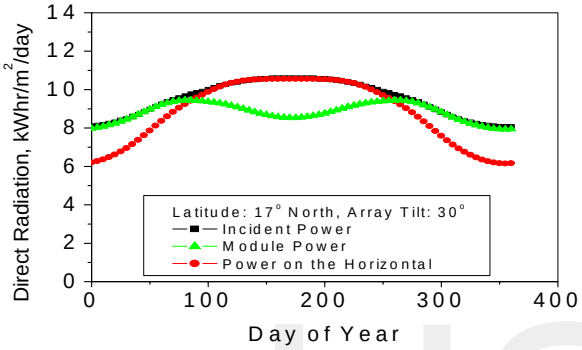

Cont. Fig. (18): Direct solar radiation vs. day of year, plotted at different latitude-and arrays angles.

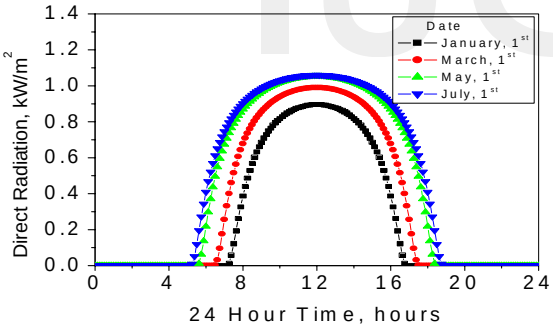

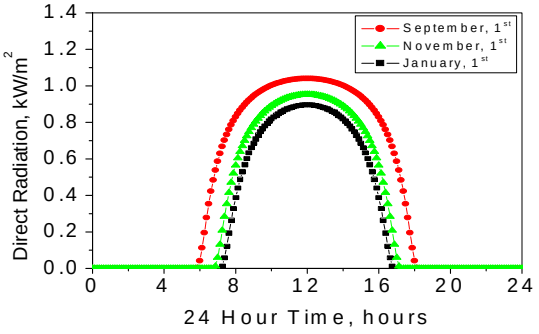

Fig. 19. Solar direct radiation vs. 24 hour day time, plotted at different year months.

Figure (20) shows the intensity of direct radiation, at Cairo, in kW/m² throughout the day. It is the amount of power that would be received by a tracking concentrator in the absence of cloud. The time is the local solar time.

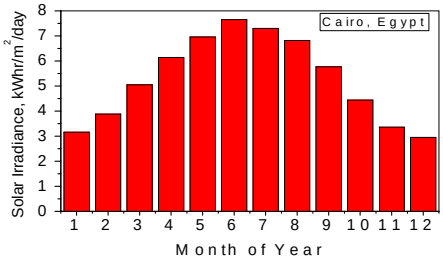

Fig. 20. Output power in kWhr/m2/day at Cairo, Egypt, plotted at different months of the year .

8 Solar Irradiance

Solar Irradiance is a measure of how much solar power you are getting at your location. This irradiance varies throughout the year depending on the seasons. It also varies throughout the day, depending on the position of the sun in the sky, and the weather. The irradiance calculator takes data collated over a 22 year period to provide monthly average insolation figures. This infor-mation is then used to calculate the average daily power generation a photovoltaic system will produce in any given month. In this concern, Fig. (21) shows the output power of solar panel in kWhr/m2/day set at different angles at (a) Cairo, Egypt, (b) Al-Arish, Egypt, and (c) Aswan, Egypt, plotted at different months of the year [19].

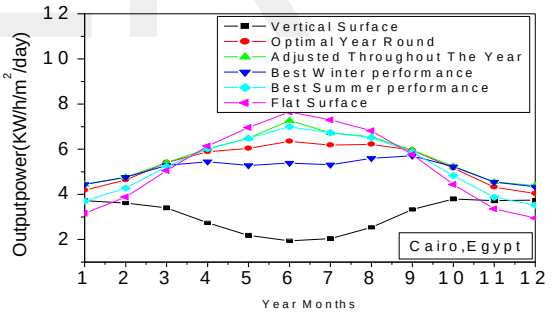

(a)

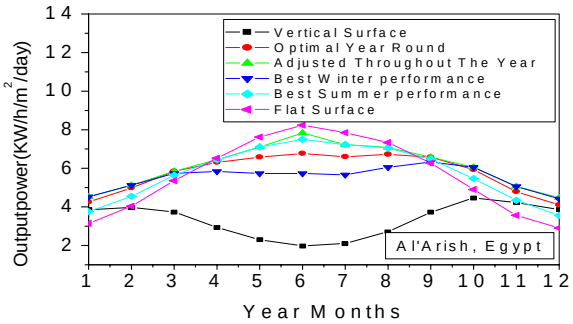

(b)

IJSER © 2016
http://www.ijser.org

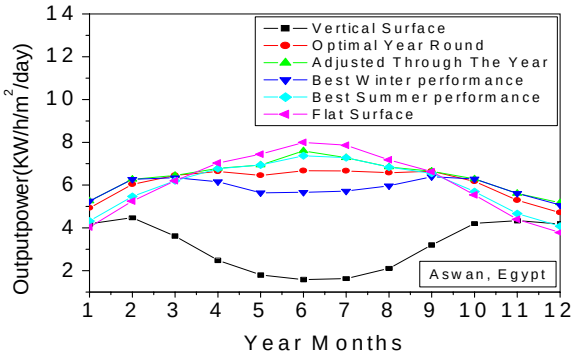

(c)

Fig. 21. Output power of solar panel, in kWhr/m2/day, set at different angles at (a) Cairo, Egypt, (b) Al'Arish, Egypt, and (c) Aswan, Egypt, plotted at different months of the year.

CONCLUSIONS

From the study, results, and analysis, compared with the previously published experi-mental results by the authors and others, it is proved that computer simulations are of great benefit as a rapid, and accurate tools. The work could be considered as a simple tool for photovoltaic and solar energy researcher.

REFERENCES

[1] PVEeducation.org / pvcdrom / characterisation / introduction-to-simulation.
[2] PVEducation.org / pvcdrom / characterisation / pc1d.
[3] R.K. Nema, S. Nema, and G. Agnihotri, "Computer Simulation Based Study of Photovoltaic Cells / Modules and their Experimental Verification ", Intr. Journal of Recent Trends in Engineering, Vol. 1, No. 3, May 2009.
[4] M. Edouardm and Donatin NJOMO, "Mathematical Modeling and Digital Simulation of PV Solar Panel using MATLAB Software ", Intr. Journal of Emerging Technology and Advanced Engineering, Vol. 3, No. 9, Sept. 24, 2013.
[5] W.Keogh and A.Blakers, "Natural Sunlight Calibration of Silicon Solar Cells", 17th European Photovoltaic Solar Energy Conference, 2001.
[6] K.Emery, et al., " Solar simulation-problems and solutions", 20th IEEE PV Specialists Conference, 1988 :1087.
[7] Heliotronics.com/papers/EDUCATION.pdf.
[8] pveducation.org/pvcdrom/characterisation/pc1d.
[9] M. Chegaar, et al., "Effect of Illumination Intensity on Solar Cells Parameters", Terra-Green 13th Intr. Conf. 2013 -Advancements in Renewable Energy and Clean Environment, Energy Procedia, Vol. 36, pp. 722–729, 2013.
[10] Firoz Khan, "Effect of illumination intensity on cell parameters of a silicon solar cell", Solar Energy Materials and Solar Cells, Vol. 94, No. 9, pp. 1473-1476. Sept. 2010.
[11] M.S.I. Rageh, M.M. Seddik, F.A.S. Soliman, A.Z. El-Behay, and M. Marzok Ibrahim,"Characteristics of photovoltaic Solar Cells", 8th Conf. on Solid-State Sci's. and Appl's., EL-Minia Univ., EL-Minia, Egypt, 24-27 February 1985.
[12] F.A.S. Soliman, M. El-Fouly and M. El-Ashry, "Photovoltaic Devices: Simulation, Properties and the Effect of Physical Parameters ", Intr. Jr. of Perspectives in Energy, Moscow Intr. Center, Russia, Printed at Pion Publisher, Ltd., U.K., Vol. 3, pp. 35-46, Oct. 1995.
[13] S.M. El-Ghanam , W. Abd El-Basit, and F. A. S. Soliman, "Simulating of the Silicon Photovoltaic's Operation at Outer Space Environments", Journal of Advancement in Science and Technology Research (ASTR), Vol. 2, No. 3, pp. 42-53, July 2015.
[14] International Renewable Energy Agency; IRENA, "Concentrating Solar Power", Vol. 1, No.2/5, June 2012.
[15] W.J.Yang, "Internal quantum efficiency for solar cells", Solar Energy, Vol. 82, No. 2, pp. 106-110, February 2008.
[16] N. M. Ranvindra, " Analysis of series and shunt resistance in silicon solar cells using single and double exponential models", Emerging Materials Research 02/2012; Vol. 1, No. 1, pp. 33–38. DOI: 10.1680/emr.11.00008
[17] A. Dhass, "Influence of shunt resistance on the performance of solar photovoltaic cell", Intr. Conference on (ICETEEEM), 2012, pp. 382-386, 13-15 Dec. 2012.
[18] Soha M. Abd El-Azeem, "Novel Techniques for Improvement of Solar Energy Conversions ", M.Sc. Thesis, Faculty of Girls, Ain-Shams University, Cairo, Egypt, June 2014. Supervised by: F.A.S. Soliman, S.A. Kamh, and S.M. El-Ghanam.
[19] F.A.S. Soliman, " Measurements of Solar Radiation in Egypt During the Period 1982- 1987", 1st Intr. Conf. on Re–Newable Energy Sources, Cairo, Egypt, 13-16 June 1988, Vol. 1, pp. 379-387.

IJSER © 2016
http://www.ijser.org